City Research Online

City, University of London Institutional Repository

Citation: Chen, X., Wan, D-W., Jin, L-Z., Qian, K. & Fu, F. (2019). Experimental studies and Microstructure Analysis for Ultra High-Performance Reactive Powder Concrete. Construction and Building Materials, 229, 116924. doi: 10.1016/j.conbuildmat.2019.116924

This is the accepted version of the paper.

This version of the publication may differ from the final published version.

Permanent repository link: https://openaccess.city.ac.uk/id/eprint/22779/

Link to published version: https://doi.org/10.1016/j.conbuildmat.2019.116924

Copyright: City Research Online aims to make research outputs of City, University of London available to a wider audience. Copyright and Moral Rights remain with the author(s) and/or copyright holders. URLs from City Research Online may be freely distributed and linked to.

Reuse: Copies of full items can be used for personal research or study, educational, or not-for-profit purposes without prior permission or charge. Provided that the authors, title and full bibliographic details are credited, a hyperlink and/or URL is given for the original metadata page and the content is not changed in any way.

City Research Online: http://openaccess.city.ac.uk/ publications@city.ac.uk

*Revised Manuscript
Click here to view linked References

Experimental studies and Microstructure Analysis for Ultra High-Performance Reactive Powder Concrete

Xuan Chen[1,2] Dong-wei Wan[3] Ling-zhi Jin[1] Kai Qian[1] Feng Fu[1.4*]

[1] College of Civil Engineering and Architecture, Guilin University of Technology, China, 541004

[2] Audit Office, Guilin University of Aerospace Technology, China, 541004

[3] Capital Construction Division, Guilin University of Electronic Technology, China, 541004

[4] School of Mathematics, Computer Science and Engineering, City, University of London, London, EC1V 0HB, U.K. (Corresponding author)

Abstract: In this paper, the strengthening mechanism of curing temperature, fine aggregate gradation, reactive materials, water reducer type, dosage and types of fibers on the microstructures and mechanical properties of Ultra-high-Performance Concrete (UHPC) was analyzed in detail by means of microstructure analysis using Scanning Electron Microscope (SEM) and mechanical tests. Based on the mechanical tests and analysis of the microstructure, a new optimal mix proportion of UHPC was also developed by considering the economic benefits. It is found that the gradation of UHPC fine aggregate can achieve the densest stacking state gradation after the optimization of mix proportion. Gradation Optimization promotes UHPC to be hydrated step by step. A large amount of hydrated calcium silicate (C-S-H) gel and a small amount of crystal produced in the early hydration phase together form the original structure of the concrete. The initial hydration products consume a large amount of Ca $(OH)_2$ to produce C-S-H and other cementitious substances by so called Secondary Hydration Reaction, the C-S-H can further catalyst hydration. It is also found that the low water-cement ratio can reduce porosity and improve the compactness and compressive strength of UHPC microstructure. The fibers can effectively delay the appearance and development of micro-cracks in the concrete matrix, help to improve the toughness, ductility and flexural properties of UHPC, and avoid brittle failure. High temperature curing is beneficial to the formation of cementitious substances with lower calcium-silicate ratio (C/S) and catalyst the occurrence of secondary hydration reaction.

Key words: UHPC; mechanical properties; microstructure; C-S-H; secondary hydration reaction

* Corresponding author: E-mail address: cenffu@yahoo.co.uk

1. Introduction

In order to obtain ultra-high performance concrete, the basic principle and main method are to reduce porosity, optimize pore structure, improve compactness and addition of extra fiber[1][2]. Taking reactive powder concrete as an example, it effectively combines the uniformly distributed ultrafine particle and the fiber reinforcement material. In its microstructure, UHPC is a composition of multi-scale composite material such as fine aggregate, cement and pores. The macroscopic mechanical properties of UHPC are largely influenced by the internal microstructure, which is closely related to the composition, mix ratio and preparation process of raw materials. Therefore, increasing research has been conducted on well-chosen selection of raw materials, use of common technology, and their influences on the microstructural characteristics, mechanical properties and durability of UHPC to facilitate the production and applications of UHPC [3][4]. The related materials include Nano silica [5][6], finely ground or sorted super fine fly ash, super fine mineral powder, super fine cement [7], metakaolin [8][9], etc. Ahmad et al. [10] and Xie et al. [11] changed raw materials and adjusting the proportion of ingredients. Park and Kang [12], Richard and Cheyrezy [13] and Granger et al. [14] also found that incorporation of these materials into UHPC not only fulfills the economic requirement, but also brings other advantages such as lowering the shrinkage and improving the mechanical properties and durability of concrete. In addition, Bornemann et al.[15] explained the improvement of tensile strength of UHPC with steel fibers by means of microstructures. Urs Müller et al.[16] and Sung-Hoon K et al.[17] studied the microstructure of UHPC using electron microscopy, and explored the effects of HT temperature and duration on the hydration reaction, microstructure, and mechanical properties of UHPC.

Until now, applications of UHPC in many countries have been reported [18][19][20].The enhanced mechanical properties and durability of UHPC also has been widely reported [21][22][23][24]. But there is still a lack of systematic microstructure analysis and mechanical property investigation of UHPC. Therefore, in this paper, the microstructure and mechanical property of UHPC are analyzed in detail by means of electron microscopy and mechanical properties tests. The main factors

affecting the properties of UHPC, such as curing temperature, fine aggregate gradation, reactive materials, water reducer, types and dosage of fibers are studied, their strengthen mechanism to the UHPC was investigated in detail and the new way to optimize the mix design is developed.

2. Material and Specimen preparation

At present, there is no mature theory on mix proportion design of UHPC. The Chinese code "Reactive Powder Concrete" (GB/T 31387-2015)[25] only specifies the water-to-cement ratio, the amount of cementitious material and the recommended dosage of steel fiber. In preparation of UHPC, the mix proportion of UHPC is mainly decided by three aspects: the selection of reactive materials, the type and dosage of fibers, and the gradation of fine aggregates. In preparation of the mix, the high Range Water Reducer (HRWR) was used to achieve a better dispersion of reactive powder and fibre in aqueous solution.

2.1 Composition of materials

1) cement

The 42.5 grade ordinary Portland cement commonly used in the market was selected for the test. The main performance indicators are shown in Table 2.1. The source of cement is Guangxi Xingan Conch Cement Co., Ltd.

Table 2.1 Main performance indicators of cement

cement fineness (cm^2/g)	initial setting time (min)	final setting time (min)	water requirement of normal consistency	loss on ignition
3400	160	220	27%	0.5

2) silica fume

The main technical indexes of silica fume are shown in Table 2.2. The source of silica fume is Guangxi Liuzhou OVM Company.

Table 2.2 Chemical composition of silica fume

test items	SiO_2	Fe_2O_3	Al_2O_3	CaO	MgO	K_2O	Na_2O	SO_3
mass percentage(%)	82.22	1.81	0.97	0.36	1.31	0.84	0.16	0.27

3) silicon powder

The main technical indexes of silicon powder are shown in Table 2.3. The source of silicon powder is Guangxi Liuzhou OVM Company.

Table 2.3 Chemical composition of silicon powder

test items	SiO_2	Al_2O_3	Fe_2O_3	CaO	MgO	Other items
mass percentage(%)	96.47	0.15	0.13	0.13	0.02	2.01

4) quartz powder

Quartz powder is a hard and wear-resistant silicate mineral with a pale yellow appearance. The average particle size of quartz powder used in the experiment is 10 micron. The content of SiO_2 in quartz powder is not less than 99%. The source of quartz powder is Guangxi Liuzhou OVM Company.

5) fly ash

The main technical indexes of fly ash are shown in Table 2.4. The source of fly ash is Guangxi Liuzhou OVM Company.

Table 2.4 Chemical composition of fly ash

test items	SiO_2	Al_2O_3	Fe_2O_3	CaO	MgO	$K_2O + Na_2O$	Other items
mass percentage(%)	52.7	25.8	9.7	3.7	1.2	2.3	4.6

2.~~1~~2 Selection of reactive powder

On the basic of the UHPC mix proportion proposed by Zheng et al. [26], the proportion of silica fume, silicon powder, quartz powder, fly ash and other mineral fine aggregate are determined. The optimized mix proportion is shown in Table 2.5.

Table 2.5 Mix proportion optimization of active materials

number	cement	Quartz sand	silica fume	silicon powder	quartz powder	Fly ash	Steel fibre /%	Subgroup	water	Water reducer
A1	1	1.1	0.35	0	0	0	0.1	0.1	0.2	0.015
B1	1	1.1	0.28	0.07	0	0	0.1	0.1	0.2	0.015
B2	1	1.1	0.21	0.14	0	0	0.1	0.1	0.2	0.015
B3	1	1.1	0.14	0.21	0	0	0.1	0.1	0.2	0.015
B4	1	1.1	0.07	0.28	0	0	0.1	0.1	0.2	0.015
B5	1	1.1	0	0.35	0	0	0.1	0.1	0.2	0.015
C1	1	1.1	0.28	0	0.07	0	0.1	0.1	0.2	0.015
C2	1	1.1	0.21	0	0.14	0	0.1	0.1	0.2	0.015
C3	1	1.1	0.14	0	0.21	0	0.1	0.1	0.2	0.015
D1	1	1.1	0.28	0	0	0.07	0.1	0.1	0.2	0.015
D2	1	1.1	0.21	0	0	0.14	0.1	0.1	0.2	0.015
D3	1	1.1	0.14	0	0	0.21	0.1	0.1	0.2	0.015
E1	1	1.1	0.28	0	0.07	0	0.1	0.1	0.2	0.015
E2	1	1.1	0.21	0	0.07	0.07	0.1	0.1	0.2	0.015
E3	1	1.1	0.14	0	0.07	0.14	0.1	0.1	0.2	0.015

Note: Proportion A: benchmark proportion, only silica fume; Proportion B: change the content of silica powder on the basis of Proportion A; Proportion C: change the content of silica powder on the basis of Proportion A; Proportion D: change the content of fly ash on the basis of Proportion A; Proportion E: change the content of silica powder and fly ash at the same time on the basis of Proportion A. The main materials of the subgroup include polyester fibers, Expansion agent and latex proteins. The quantity of cement in concrete is 998kg/m^3.

2.~~2~~3 Type of the steel fiber and dosage

In order to optimize the type and content of fibers, three types of fibers were used in the UHPC mix design: steel fiber, polypropylene fiber and hybrid fiber with both steel fiber and polypropylene fiber. The optimum mix ratio of UHPC fiber type

and content is shown in Table 2.6.

Table 2.~~2~~6 Mix proportion of fiber types and dosage

number	cement	Quartz sand,	silica fume,	quartz powder	silica powder	Steel fibre	polypropylene fiber	Reducer catalyst	Water reducer	Water
A1	1	0.9	0.35	0.2	0.35	0	0	0.1	0.015	0.28
B1	1	0.9	0.35	0.2	0.35	1%	0	0.1	0.015	0.28
B2	1	0.9	0.35	0.2	0.35	2%	0	0.1	0.015	0.28
B3	1	0.9	0.35	0.2	0.35	3%	0	0.1	0.015	0.28
C1	1	0.9	0.35	0.2	0.35	0	0.2%	0.1	0.015	0.28
C2	1	0.9	0.35	0.2	0.35	0	0.3%	0.1	0.015	0.28
C3	1	0.9	0.35	0.2	0.35	0	0.4%	0.1	0.015	0.28
D1	1	0.9	0.35	0.2	0.35	1%	0.2%	0.1	0.015	0.28
D2	1	0.9	0.35	0.2	0.35	1%	0.3%	0.1	0.015	0.28
D3	1	0.9	0.35	0.2	0.35	1%	0.4%	0.1	0.015	0.28
E1	1	0.9	0.35	0.2	0.35	2%	0.2%	0.1	0.015	0.28
E2	1	0.9	0.35	0.2	0.35	2%	0.3%	0.1	0.015	0.28
E3	1	0.9	0.35	0.2	0.35	2%	0.4%	0.1	0.015	0.28
F1	1	0.9	0.35	0.2	0.35	3%	0.2%	0.1	0.015	0.28
F2	1	0.9	0.35	0.2	0.35	3%	0.3%	0.1	0.015	0.28
F3	1	0.9	0.35	0.2	0.35	3%	0.4%	0.1	0.015	0.28

Note: Steel fiber is volume ratio, the rest is mass ratio.

Proportion A: benchmark ratio, without any fibers; Proportion B: change steel fiber content on the basis of Proportion A; Proportion C: change polypropylene fiber content on the basis of Proportion A; Proportion D: add 1% steel fiber on the basis of Proportion A, change polypropylene fiber content; Proportion E: add 2% steel fiber on the basis of Proportion A, change polypropylene fiber content; Proportion F on the basis of Proportion A, change polypropylene fiber content and add 3% steel fibers. The quantity of cement in concrete is 998kg/m^3.

2.~~3~~4 Gradation of fine aggregate

In accordance to reference [21], the recommended water-cement ratio, amount of cementitious materials and dosage of steel fibers and three fine aggregate gradation

were initially determined based on the principle of Close-packed structures, as shown in Table 2.~~3~~7.

Table 2.~~3~~7 Mix proportion of fine aggregate gradation

Number	Cement	Quartz sand			Silica fume	Fly Ash	Steel fiber	Water reducer	Water
		Coarse	Medium	Fine					
1	1	0.20	0.80	0.20	0.30	0	2%	0.02	0.23
2	1	0.23	0.94	0.23	0.25	0	2%	0.05	0.25
3	1	0.28	1.20	0.28	0.15	0.09	2%	0.05	0.25

Note: The quantity of cement in concrete is 998kg/m^3.

2.~~4~~5 Casting and curing

UHPC has high viscosity and poor liquidity. The use of high-power dispenser can disperse the viscous slurry evenly, drive away the air, and solve the problem of fiber clumping. The mixing and maintenance process of UHPC is shown in Figure 2.1.

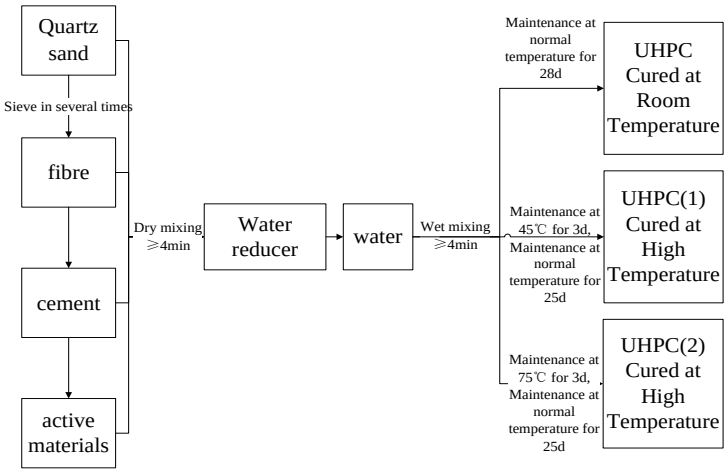

Fig 2.1 Flow chart of Mixing and curing UHPC

3. Material tests

The effects of curing temperature, fine aggregate gradation and active material on the mechanical properties of UHPC were investigated by compressive strength test,

splitting tensile strength test, flexural strength test and chloride ion (Cl^-) permeability test.

3.1 Compressive strength test, splitting tensile strength test, flexural strength test

The compressive strength test was carried out by the electronic-hydraulic servo pressure testing machine controlled by YAW-3000D microcomputer. The bearing surface of the specimen is parallel to the pouring direction and is loaded at a uniform speed of 1.2 MPa/s. The specimen placed in the splitting tensile strength test is the same as that in the cube compression test, and is loaded at a uniform speed of 0.12 MPa/s. The bending strength test is carried out by four-point bending test and loading at a uniform speed of 0.08 MPa/s. The specific dimensions of test pieces are shown in Table 3.1.

Table 3.1 The specific dimensions of test pieces

Number	Mechanical property index	size
1	Cube compressive strength	100mm×100mm×100mm
2	Axial compressive strength	100mm×100mm×300mm
3	splitting tensile strength	100mm×100mm×100mm
4	Flexural strength	100mm×100mm×400mm

3.2. chloride penetrability test

The permeability of chloride ion (Cl^-) was tested by salt-saturated concrete conductivity method (also known as NEL method)[27]. The main principle is that the specimen is made into "electrical element" (containing only conductive particle Cl^-) by vacuum and salt treatment, and then the conductivity of the specimen is measured in DC electric field, and the chloride ion diffusion coefficient is determined by Nernst-Einstein equation. The chloride penetrability of concrete was determined following the procedures of ASTM C1202-94 using the 50-mm thick portions as sample obtained from the 100 by 200 mm concrete cylinders. The resistance of concrete against chloride ion penetration is expressed as an electrical indication: the total charge passed in coulombs during a test period of 6 h.

4. Material Tests results and discussion

4.1 Effect of Reactive Materials on cubic Compressive Strength and Permeability of chloride ion (Cl^-)

As shown in Figure 4.1, the cubic compressive strength of UHPC decreases with the increase of substitution ratio of silica powder, quartz powder, and fly ash. The chemical composition of silica powder is similar to that of silica fume, but the particle size is between silica fume and cement, and the degree of secondary hydration reaction is lower than that of silica fume, so the reactivity of silica fume is slightly poor and its water usage is also increased, which leads to the reduction of cubic compressive strength. The main component of quartz powder is SiO_2, but it can only achieve its largest reactivity when the curing temperature reaches 200 ~250 C^o. The highest curing temperature in this experiment is maintained at 75 ~5 C^o, so the pozzolanic activity of quartz powder has not been fully stimulated. With the increase of fly ash replacement ratio, the cubic compressive strength of UHPC increases or decreases, but when the replacement ratio reaches 40%, the cubic compressive strength reaches its maximum value, which indicates that the reactivity of fly ash is similar to that of silica fume and can effectively improve the strength of UHPC. However, the spherical surface of fly ash is compact and stable, it is not easy to hydrate, and the reactivity may need longer time. When quartz powder and fly ash are mixed together, the cubic compressive strength decreases, but the decrease is much smaller than that of quartz powder or fly ash alone, because the two materials can complement each other.

From Figure 4.2, it can be seen that the Cl-permeability coefficient of UHPC increases with the increase of replacement ratio of silica powder and quartz powder and decreases with the increase of replacement ratio of fly ash, mixture of quartz powder and fly ash. The permeability of four specimens can reach grade IV, and the permeability of UHPC is low. According to the theory of diffuse double layer[28], slurry hydration products can only absorb charged ions and form compact and diffuse layers at the interface of capillary pore. The double layer will affect Cl-diffusion. The premise of Cl-diffusion is to have sufficient diffusion force to break away the repulsion between the two layers. When the relative capillary aperture of UHPC (the

thickness of the two layers) is smaller, the two layers will be separated. The greater the repulsive force is, the stronger the restraint to Cl-is, which is also the reason for the smallest Cl-Permeability coefficient of fly ash.

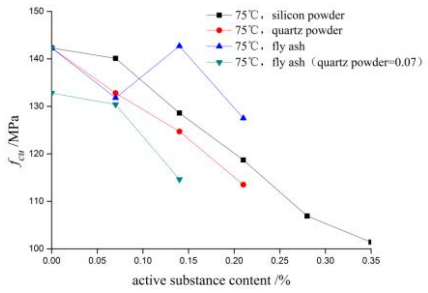

Fig 4.1 Effect on compressive strength

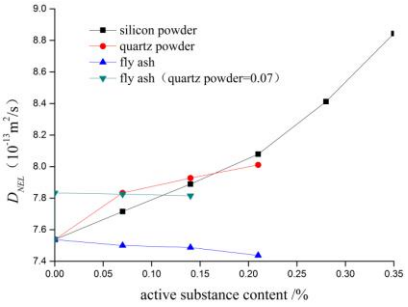

Fig 4.2 Effect on chloride ion permeability

4.2 Effect of Fiber Type and Dosage on Cubic Compressive Strength, Splitting Tensile Strength and Cl-Permeability

From Figs. 4.3, 4.5 and 4.7, it can be seen that the cubic compressive strength, splitting tensile strength and Cl-Permeability of UHPC increase with the increase of dosage of steel fibers. When the dosage of steel fibers is 2%, the cubic compressive strength and splitting tensile strength of UHPC reach their peak values, and the growth of Cl-permeability begins to slow down. With the increase of dosage of steel fibers, the compressive and tensile failure modes of UHPC specimens gradually change from brittle failure to ductile failure, and the cohesion and friction of materials increase. The steel fibers help the closure of cracks, hence, to resist the energy released from cracks. The increase of dosage of steel fibers requires more slurry inclusion filling, and the more the volume fraction, the easier the agglomeration, resulting in the increase of internal porosity and the increase of Cl-permeability. However, the toughening effect of steel fibers reduced, therefore, the permeability of UHPC can still reach grade IV with low permeability.

From Figs. 4.4, 4.6 and 4.8, it can be seen that, with the increase of dosage of fibers, polypropylene fibers have no significant effect on cubic compressive strength, splitting tensile strength and cl-permeability. Polypropylene fiber has low elastic modulus, and small dosage of polypropylene fibers were added in this test, and their restraint effect on cement structural matrix only work in the early stage of cement

hardening, so the cracks formation delay is not obvious.

The compressive strength and splitting tensile strength of mixed type of fibers are obviously higher than those of single type fibers. The compressive strength and splitting tensile strength of mixed fibers with high steel fiber content are generally higher than those with low steel fiber content. The peak value of cubic compressive strength occurs when the dosage of steel fibers is 2%. Because the two kinds of fibers complement to each other and reinforce each other, concrete becomes more compact, therefore, the Cl permeability of UHPC is reduced.

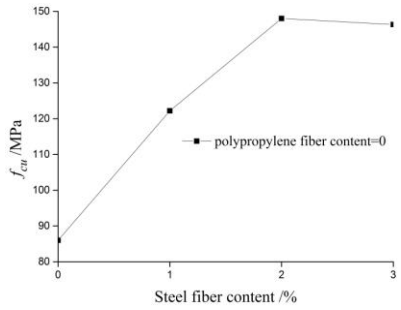

Fig 4.3 Steel fiber dosage- compressive strength

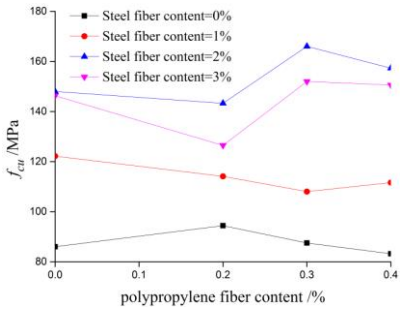

Fig 4.4 Polypropylene fiber dosage-compressive strength

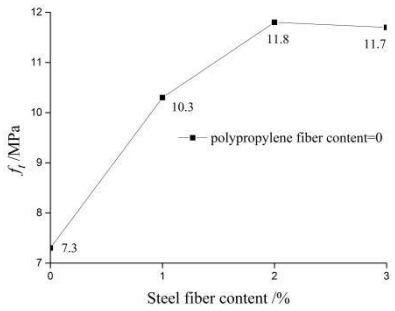

Fig 4.5 Steel fiber dosage- tensile strength

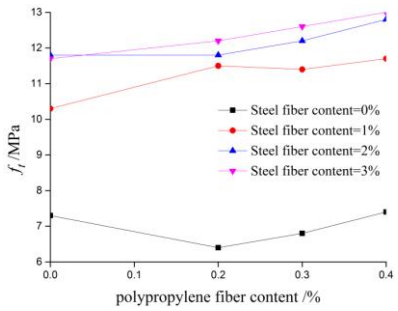

Fig 4.6 Polypropylene fiber dosage- tensile strength

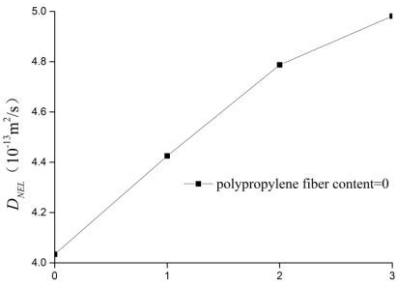

Steel fiber content %

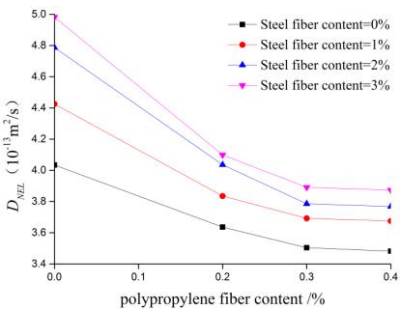

Fig 4.7 Steel fiber content dosage- Ci permeability Fig 4.8 Polypropylene fiber dosage-chloride ion permeability

4.3 Effect of Fine Aggregate Gradation on Basic Mechanical Properties

From Figure 4.9, it can be seen that the cubic compressive strength, cylindrical compressive strength and tensile splitting strength of mix 1 are all greater than those of mix 2 and 3. In order to obtain higher compact density, it is necessary to consider the gradation of cementitious composite actions. Mix 1 reduces the amount of quartz sand, increases the amount of silica fume, decreases the water-cement ratio, and increases the plastic viscosity and ultimate shear stress of cement. According to rheological principle, the greater the ultimate shear stress of mixtures, the smaller the fluidity of mixtures, because the distance between cement particles decreases at this time, and the force between particles increases. Therefore, in order to control the water-cement ratio, it is necessary to increase the dosage of water reducer in order to obtain sufficient fluidity, but the experiment proves that increasing the dosage of water reducer cannot offset the decrease of fluidity caused by the decrease of the dosage of cementitious materials.

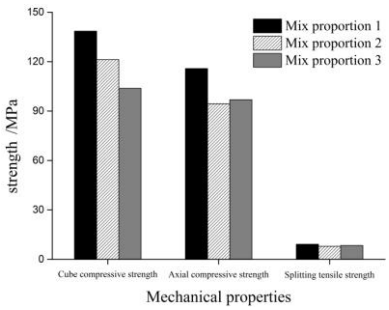

Fig 4.9 Effect of fine aggregate gradation on basic mechanical properties

4.4 Effect of curing methods on cubic compressive strength and Cl-Permeability

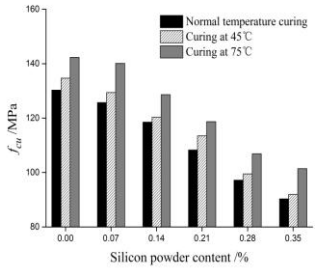

Fig 4.10 Compressive strength (silicon powder)

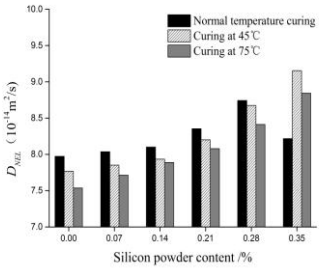

Fig 4.11 Ci permeability (silicon powder)

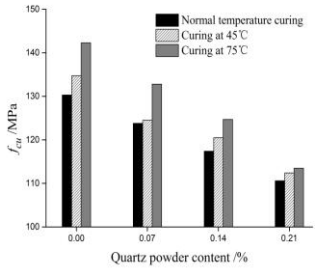

Fig 4.12 Curing mode-compressive strength (quartz powder)

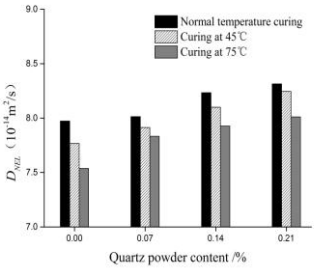

Fig 4.13 Curing mode-Ci permeability (quartz powder)

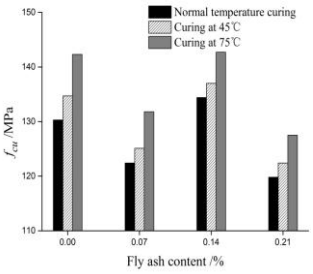

Fig 4.14 Curing mode-compressive strength (fly ash)

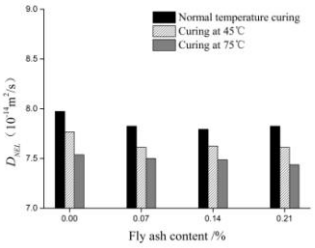

Fig 4.15 Curing mode-Chloride ion permeability (fly ash)

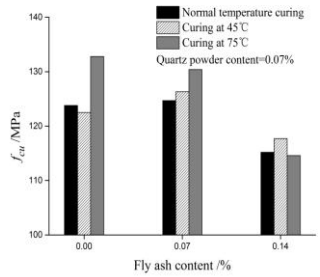

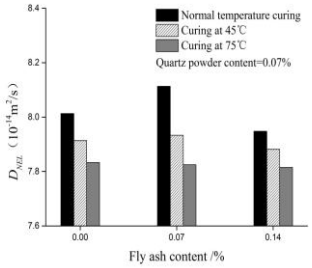

Fig 4.16 Curing mode- compressive strength (mixed fiber) Fig 4.17 Curing mode-Ci permeability (mixed fiber)

From Fig. 4.10-4.17, it can be seen that, the cubic compressive strength of UHPC with silica powder, quartz powder and fly ash increases obviously under thermal curing condition, especially the improvement of curing condition at 75 is much greater than that at $45^{o}C$. The cubic compressive strength with mixed quartz powder and fly ash increases. It is indicated that the increase of curing temperature can stimulate the pozzolanic effect of reactive materials. The higher the degree of hydration reaction occurs, the more C-S-H is produced, the density of slurry increases, and the cubic compressive strength increases. The curing method also had an effect on the Cl- permeability of UHPC. With the increase of curing temperature, the permeability coefficient of Cl- in several blocks decreased significantly, and the C-S-H increased the density of the slurry. Water conservation also reduced the evaporation of UHPC capillary pores to a certain extent and continued to replenish water. The hydration of the pulp continued and contracted, and the more thoroughly the hydration, the less the pores of the slurry, the smaller the permeability coefficient of Ci.

5. Microstructure analysis of UHPC

To gain further insight of the effective mix proportion for UHPC, the UHPC samples were inspected by the Scanning Electron Microscopy (SEM) method at Guilin university of technology. All samples were inspected as taken from the specimen without any further processing. Below is the discussion of the effect of different parameters on the SEM observations.

5.1 Effect of the dosage of the steel fiber on the UHPC microstructure

Fig. 5.1-5.4 are the SEM morphology of UHPC microstructures with 50-10000 x magnification. From Figure 5.1, it can be seen that well-dispersed fibers are identified by observing individual fiber within the matrix without any agglomeration. The bond between steel fibers and cement in UHPC is relatively strong, and no obvious $Ca(OH)_2$ crystals are found at the fiber pull-out position. It is speculated that the interfacial zone between steel fibers and cement is filled by the product of secondary hydration reaction, and the transition interface is not obvious. The surface of the steel fiber (Fig. 5.3) can be observed to have hydrous attachment on the surface of the fiber. The hydrates are fusiform and flocculent. They belong to type I and type II C-S-H. The presence of C-S-H improves the bonding between the steel fiber and the cement, enhances the role of fiber in UHPC as a micro reinforcement material. Because the two kinds of samples were cured at room temperature, the microstructure of the two samples was mainly composed of type II C-S-H. (Fig. 5.4).

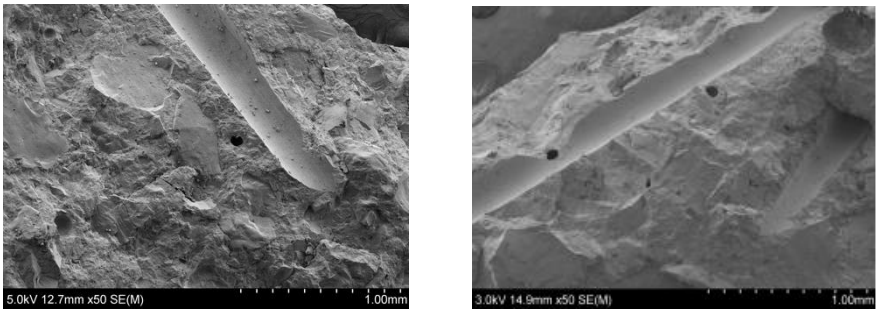

（a）Steel fiber dosage 0.75%　　（b）Steel fiber dosage 2%

Fig 5.1 UHPC microstructure observed at 50 x magnification

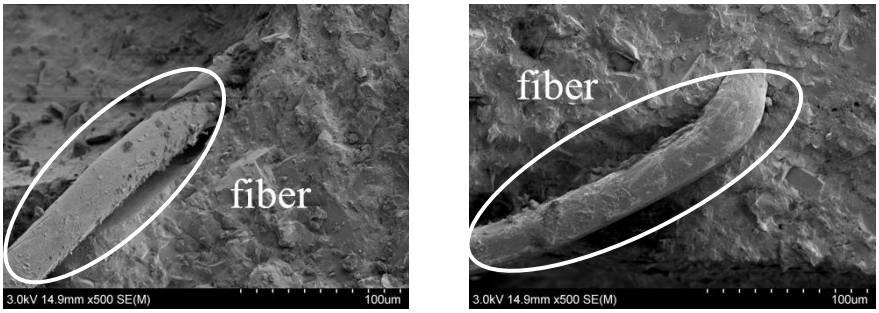

（a）Steel fiber dosage 0.75%　　（b）Steel fiber dosage 2%

Fig 5.2 UHPC microstructure observed at 500 x magnification

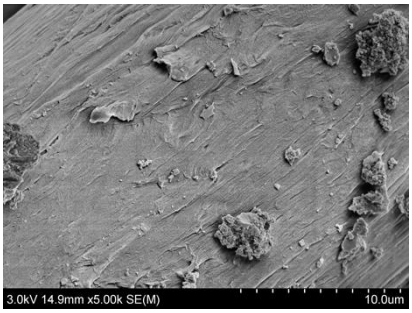

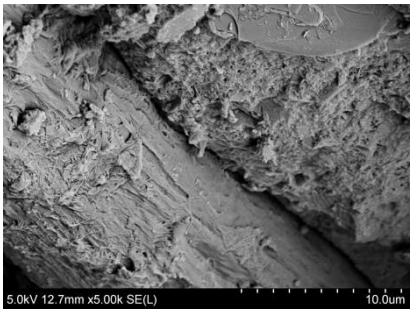

（a）Steel fiber dosage 0.75%　　（b）Steel fiber dosage 2%

Fig 5.3 UHPC microstructure observed at 5000 x magnification

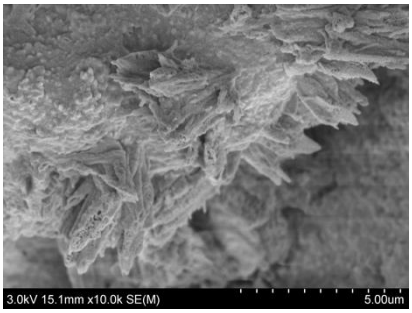

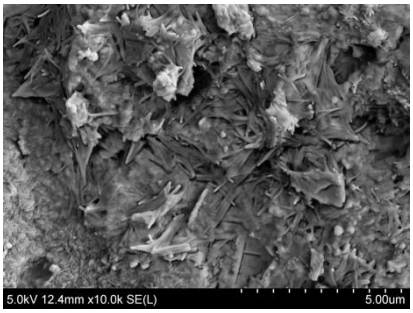

（a）Steel fiber dosage 0.75%　　（b）Steel fiber dosage 2%

Fig 5.4 UHPC microstructure observed at 10000 x magnification

5.2 Effect of fine aggregate on UHPC microstructure

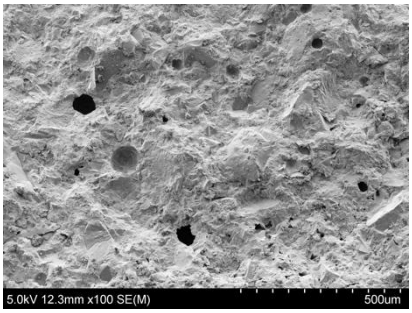

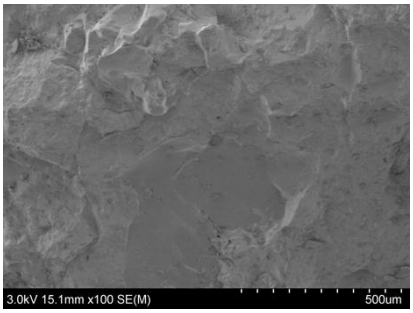

(a) non-graded quartz sand　　(b)graded quartz sand

Fig 5.5 UHPC microstructure observed at 100x magnification

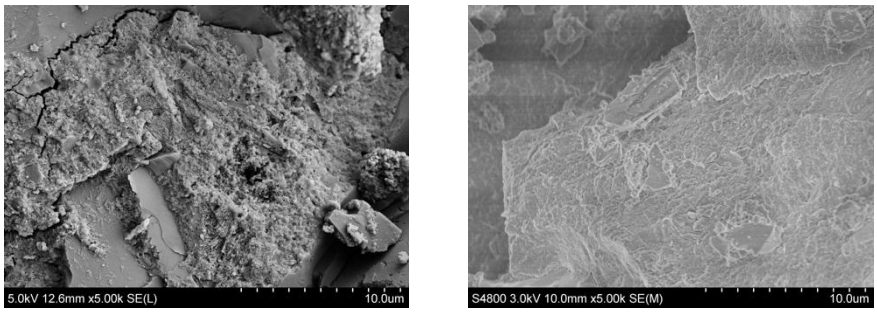

(a) non-graded quartz sand (b)graded quartz sand

Fig 5.6 UHPC microstructure observed at 5000 x magnification

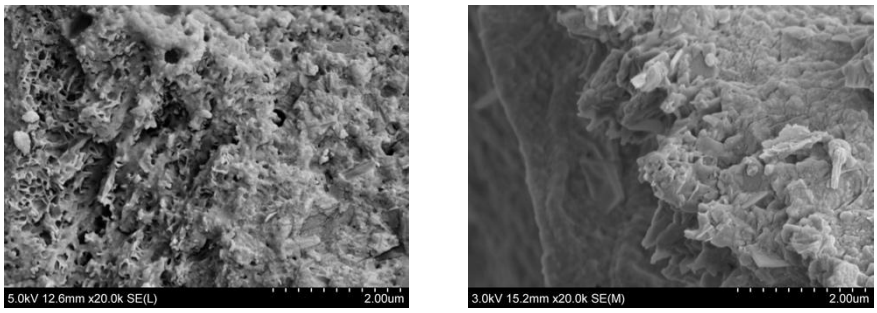

(a)non-graded quartz sand (b)graded quartz sand

Fig 5.7 UHPC microstructure observed at multiple of 20000 x magnification

Fig. 5.5-5.7 are the SEM morphology of UHPC microstructures with of 100-20000 x magnification. From Figs. 5.5 and 5.6, it can be seen that, the UHPC structure of graded quartz sand is better than that of non-graded quartz sand in microscopic homogeneity, and the voids and cracks are obviously less than those of non-graded quartz sand. The gaps between fine aggregate and cement of non-graded quartz sand structure is larger, and the cracks between them are still wider. Graded quartz sand can reasonably agglomerate dispersed aggregates, and the slurry is easier to produce mechanical interlocking force with aggregates, forming a compact fine aggregate-slurry bonding area. Although stress is easy to concentrate in the fine aggregate-slurry interface area, there will be micro-cracks at the aggregate interface, but the length of micro-cracks will be in line with the size of fine aggregate. The decrease of aggregate particles will reduce the defects and micro-cracks caused by chemical shrinkage in the initial hydration stage, and quartz powder can also react

with the initial hydration products during high temperature curing, which greatly improves the mechanical properties of cement and the elastic modulus of hardened cement, thus eliminating the non-uniformity between UHPC fine aggregate and hardened cement. As shown in figures 5.6 and 5.7, the products of the non-graded quartz sand UHPC structure are mainly a large number of particles. They belong to type II C-S-H and are formed by many interlocking within the particles which are roughly the same as the cross sections of type I particles and are doped with a little fine rod ettringite to form the skeleton of the system. The C-S-H of the graded quartz sand UHPC structure is relatively large. After high temperature curing, the products with complete hydration will fill and squeeze the limited space, and eventually gradually deposit to form a more compact internal structure. The two kinds of samples were all cured at high temperature, so the C-S-H of the two samples showed a relatively compact state.

5.3 Effect of curing method on the microstructure of UHPC

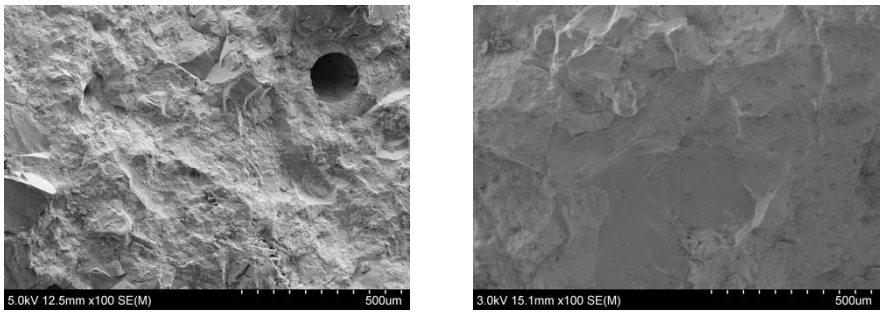

（a）Curing at Room Temperature　　（b）Curing at 75℃

Fig 5.8 UHPC microstructure observed at multiple of 100 x magnification

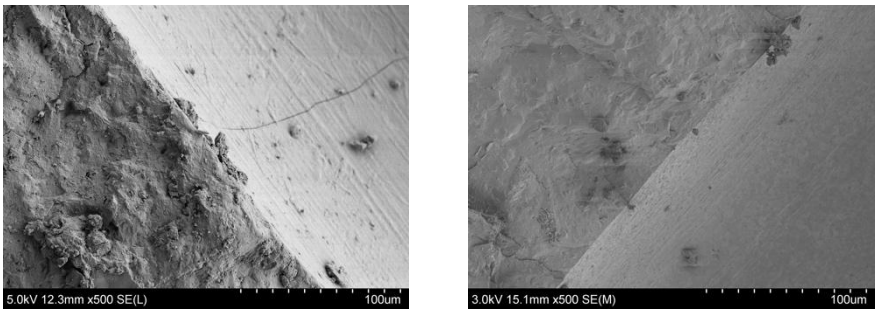

（a）Curing at Room Temperature　　（b）Curing at 75℃

Fig 5.9 UHPC microstructure observed at multiple of 500 x magnification

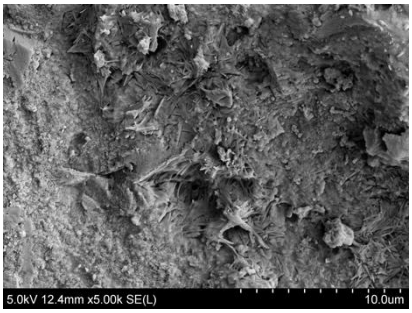

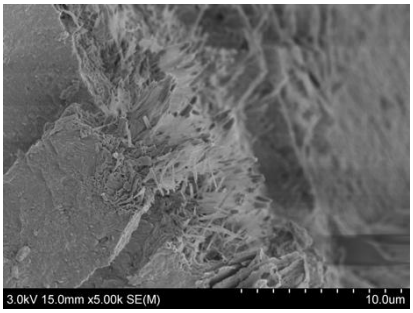

（a）Curing at Room Temperature （b）Curing at 75℃

Fig 5.10 UHPC microstructure observed at multiple of 5000 x magnification

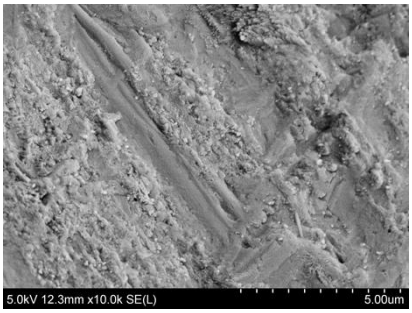

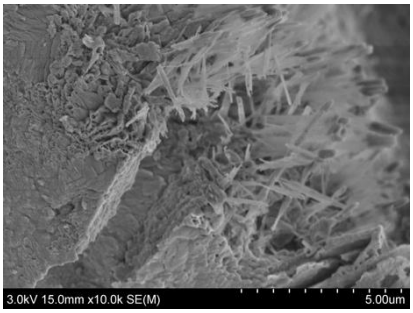

（a）Curing at Room Temperature （b）Curing at 75℃

Fig 5.11 UHPC microstructure observed at multiple of 10000 x magnification

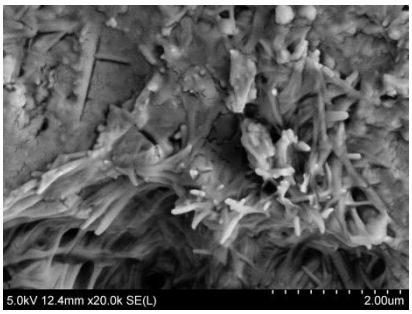

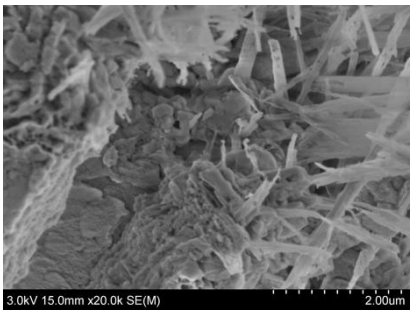

（a）Curing at Room Temperature （b）Curing at 75℃

Fig 5.12 UHPC microstructure observed at 20000 x magnification

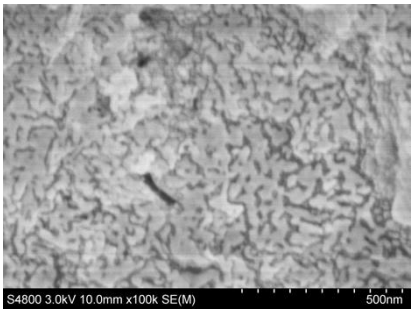

Fig 5.13 UHPC microstructure observed at multiple of 100000 magnification (Curing at 75℃)

Fig. 5.8-5.13 is the SEM morphology of UHPC microstructures with observation at 100-100 000 x magnification. According to Figure 5.8-5.9, the microstructure of the specimens cured at $75^{o}C$ is better than that cured at room temperature (the structure is looser), and the porosity, voids and cracks are obviously less than those cured at room temperature. From Fig. 5.10-5.13, it is known that the product is mainly amorphous, which contains a small amount of irregular fibrous particles. The fibrous particles belong to type I C-S-H gel. When the curing temperature rises to $75^{o}C$, the fibrous particles obviously decreases, and C-S-H shrinks, the wormlike and needle like C-S-H coexists, which is accompanied by a small number of fine rods ettringite. It can be considered that during the curing process, C-S-H will exhibit a relatively low crystallinity phase at room temperature. When the hydration temperature rises to 75 ^{o}C, the C-S-H may transform from the semi crystalline phase C-S-H (type I) to the crystalline Tobermore phase. High temperature will accelerate the hydration of clinker minerals. The C-S-H and the initial hydration product formed by high temperature accelerate the secondary hydration reaction, and the C-S-H gel will continue to adhere to the surface of the needle. The C-S-H gel will continue to grow and expand and eventually form a densely wormlike C-S-H. However, the temperature of 75 ^{o}C is not enough for the two processes of crystallization transformation and accelerated hydration. Therefore, the existence of gel phase can still be found, and the presence of other C-S-H may occur when the temperature continues to rise. This indicates that the hydration process of UHPC is the process of C-S-H growing and forming.

5.4 Effect of water reducer to the UHPC microstructure

Fig. 5.14-5.16 is the SEM morphology of UHPC microstructures with

observation at 500-20000 x magnifications. As shown in Figure 5.14, compared with the UHPC structure using Mighty High range reducer, the presence of fibers with diameter of about 200 μm can be observed, which is the polyester fibers. The main raw material of polyester fibers is polyester (PET, polyethylene terephthalate). Each fibre is independent, no agglomeration and dense bundles observed. Usually, many fibers agglomerated to form "antenna" shaped protuberance cement, which shows irregular three-dimensional distribution, and can act as a micro-reinforcement. However, due to the use of water reducer, few is formed. It was observed that the surface of the pulled out polyester fibers was smooth, there were some voids in the transition zone between the polyester fibers and the cement, and the defects were obvious. Therefore, the mechanical properties of UHPC were not significantly improved. As shown in Fig. 5.15-5.16, the C-S-H gel using the UHPC reducer catalyst appears "cloud like". The accumulation of C-S-H makes the UHPC dense inside. It can be thought that the swelling agent in the reducer catalyst and water react to produce the equal crystal, which increases the volume and continues to expand. Therefore, the network type II C-S-H should expand to form a "cloud like shape". "C-S-H" has fine pores. The C-S-H gel with UHPC structure using Mighty High Range water reducer increase the compactness of the UHPC.

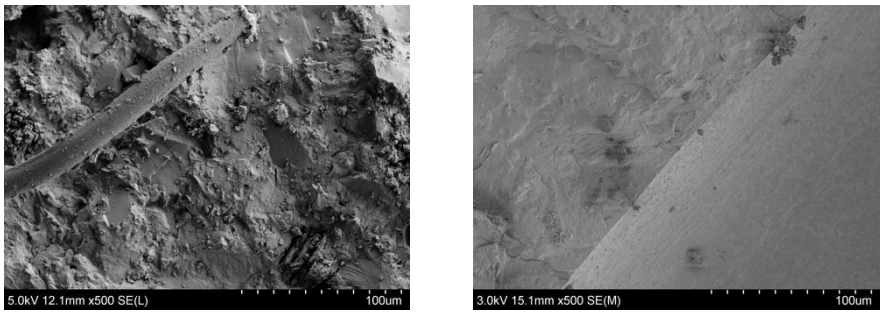

（a）Reducer catalyst　　(b)Mighty High Range reducer

Fig 5.14 UHPC microstructure observed at 500 x magnification

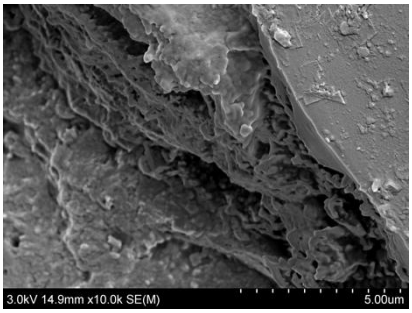

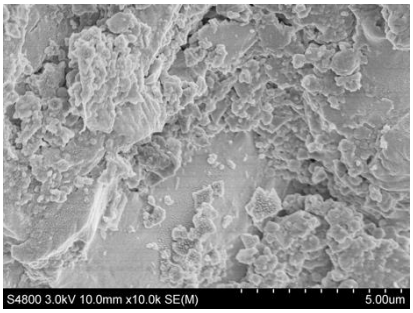

（a）Reducer catalyst （b）Mighty High Range reducer

Fig 5.15 UHPC microstructure observed at 10000 x magnification

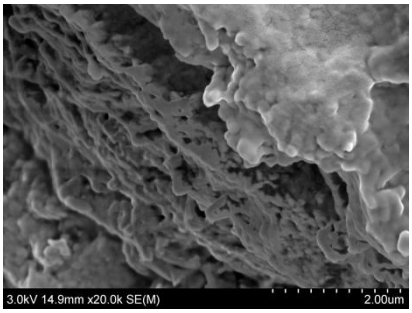

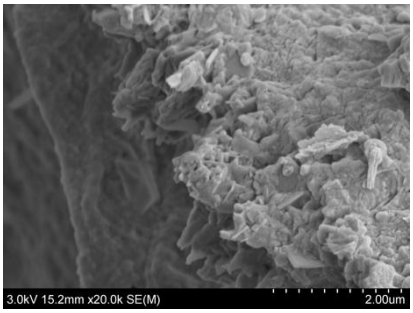

（a）Reducer catalyst （b）Mighty High Range reducer

Fig 5.16 UHPC microstructure observed at 20000 x magnification

5.5 Characteristic of UHPC microstructure

According to the microstructure analysis results of UHPC, it can be concluded that UHPC has the following microstructural characteristics:

1) UHPC has relatively low water component and good in grading of cementitious material. During hydration, a large amount of C-S-H and other cementitious materials will be generated. The structure is dense, but the crystal formation are poor. The "Secondary hydration reactions" will consume more $Ca(OH)_2$, and the content of ettringite is less.

2) The cementitious material of UHPC compose of compact and un-hydrated material particles (cement and reactive admixture) to form UHPC matrix. Quartz sand and fiber as aggregate distribute evenly in the matrix, increasing the strength and toughness of UHPC. The reactive admixture works as both static compaction and

dynamic hydration filling, which effectively improves the interface area between aggregate phase and matrix phase. Increase the density and uniformity of UHPC.

3) UHPC has fewer holes after mixing optimization and high temperature curing, and the pore size is concentrated below 500 μm. Inner pore structure is mainly harmless holes.

6. Optimization design for the mix proportion

Due to the addition of reactive material and fibers, the initial cost of UHPC is relatively high, with a unit price of \$600/m^3. To resist same level of load, the size and weight of UHPC can be reduced by about 40%. Therefore, the amount of cement and aggregate used will be greatly reduced, which can reduce the consumption of materials and energy as well as transportation costs. Moreover, the addition of fibers can reduce steel bars to a certain extent, and the direct economic benefits are enormous. Indirect economic benefits include reduced construction costs, lower replacement rate and maintenance costs of UHPC, and can also speed up capital turnover. The comprehensive economic benefits are considerable, and the cost-effective ratio is much higher than that of ordinary concrete.

Considering the cubic compressive strength, axial compressive strength, splitting tensile strength, Cl-permeability and liquidity of each specimen, and considering the micro-structure and economic benefits of UHPC, A new optimal mix proportion is developed based on the microstructure analysis and mechanical tests. It is shown in Table 6.1, which is based on the above-mentioned parameters. The curing regimes is developed through synthetically considered the cubic compressive strength, Ci permeability and microstructures of UHPC to determine the curing regimes. With the increase of curing temperature, the cubic compressive strength increases obviously, the permeability coefficient of Cl- decreased significantly. The microstructure of the specimens cured at 75 ^oC is better than that cured at room temperature (the structure is looser), and the porosity, voids and cracks are obviously less than those cured at room temperature. Therefore, the curing regimes method is curing under 75C^o for 3 days with further 25 days curing under the room temperature.

Table 6.1 The optimal proportion of UHPC

Cement	Quartz sand			Silica fume	Steel fiber	Water reducer	Water
	Coarse	Medium	Fine				
1	0.20	0.80	0.20	0.30	2%	0.02	0.23

Note: Steel fiber is volume ratio, the rest is mass ratio

7. Conclusion

In this paper, the effect of curing temperature, fine aggregate gradation, reactive materials, water reducer type, dosage and types of fibers on the strength and behavior of Ultra-high-Performance Concrete (UHPC) were analyzed in detail by means of microstructure analysis using Scanning Electron Microscope (SEM) and mechanical tests, their strengthen mechanism on the behavior of UHPC is investigated. Based on the mechanical tests and analysis of the microstructure, a new optimal mix proportion of UHPC was also developed.

Below conclusions are made:

1) The cube compressive strength of UHPC decreases with the increase of the ratio of silica powder, quartz powder, quartz powder and fly ash;
2) The Cl-permeability coefficient increases with the increase of the ratio of silica powder and quartz powder and decreases with the increase of the ratio of fly ash, quartz powder and fly ash.
3) The fibers can effectively delay the appearance and development of micro-cracks in the concrete matrix, help to improve the toughness, ductility and flexural properties of UHPC, and avoid brittle failure. The cubic compressive strength, splitting tensile strength and Cl-Permeability of UHPC increase with the increase of dosage of steel fibers, while the single polypropylene fibers have no significant effect, the hybrid fibers have higher reinforcement effect than the two-single type of fiber.
4) The cube compressive strength increases obviously with the addition of silica powder, quartz powder and fly ash and high temperature curing but the effect of quartz powder and fly ash are less significant.
5) SEM analysis shows that the interface between steel fiber and cement is filled

with C-S-H which is beneficial to combination of steel fiber and slurry, increasing the toughness and cracking resistance of UHPC.

6) The graded silica sand can reasonably amalgamate the dispersed aggregate, eliminate the inhomogeneity between single aggregate and hardened cement, and produce more C-S-H.
7) Curing temperature affects C-S-H formation. High temperature curing is beneficial to the formation of cementitious substances with lower calcium-silicate ratio (C/S) and catalyst the occurrence of secondary hydration reaction.
8) Mighty High Range reducer could react with a large number of C-S-H gel to form compact structure of the concrete.
9) The initial hydration stage consumes a large amount of Ca $(OH)_2$ to produce hydrated calcium silicate (C-S-H) and other cementitious substances by so called "Secondary Hydration Reaction", the C-S-H can further catalyst hydration.
10) Low water-cement ratio can reduce porosity and improve the compactness and compressive strength of UHPC microstructure.
11) A New optimal mix proportion is developed based on the microstructure analysis and mechanical tests.

Acknowledgement

This research sponsored by National Natural Science Foundation of China (51368013) The authors wish to acknowledge the sponsors. However, any opinions, findings, conclusions and recommendations presented in this paper are those of the authors and do not necessarily reflect the views of the sponsors.

Reference

[1] Schmidt M，Fehling E.(2005). Ultra-High-Performance Concrete: Research，Development and Application in Europe. Seventh International Symposium on the

Utilization of High-Strength /High-Performance Concrete，ACI SP-288，American Concrete Institute，1 & 2.

[2] Shi C，Wu Z，Xiao J，et al. (2015). A review on ultra high performance concrete: Part I. Raw materials and mixture design. Construction and Building Materials，101:741-751.

[3] Z. Yunsheng，S. Wei，L. Sifeng，et al.(2008). Preparation of C200 green reactive powder concrete and its static-dynamic behaviors, Cem. Concr. Compos，30(9): 831-838.

[4] R.Yu ，P.Spiesz ，H.J.H.Brouwers.(2015). Development of an eco-friendly Ultra-High Performance Concrete(UHPC) with efficient cement and mineral admixtures uses. Cement & Concrete Composites，55：383-394.

[5] Jankovic K，Stankovic S，Bojovic D，et al.(2016). The Influence of nano-silica and barite aggregate on properties of ultra high performance concrete. Constr Build Mater，126：147.

[6] Gesoglu M，Guneyisi E，Asaad D S，et al.(2016). Properties of low binder ultra-high performance cementitious composites：comparison of nanosilica and microsilica. Constr Build Mater，102：706.

[7] Van V T A，Robler C，Bui DD，et al.(2014). Rice husk ash as both pozzolanic admixture and internal curing agent in ultra-high performance concrete. Cem Concr Compos，53(10)：270.

[8] Huang W，Kazemi-kamyab H，Sun W，et al.(2017). Effect of replacement of silica fume with calcined clay on the hydration and microstructural development of eco-UHPFRC. Mater Des，121：36.

[9] Norhasri M S M，Hamidah M S，Fadzil A M，et al.(2016). Inclusion of nano metakaolin as additive in ultra high performance concrete(UHPC). Constr Build Mater，127：167.

[10] Ahmad S ，Hakeem I ，Maslehuddin M.(2015). Development of an optimum

mixture of ultra-high performance concrete. Revue Franã § aise De Gã©nie Civil，20(9)：1106-1126.

[11] Xie Y，Liu B，Yin J，et al.(2002). Optimum mix parameters of high-strength self-compacting concrete with ultrapulverized fly ash. Cement & Concrete Research，32(3)：477-480.

[12] J.J Park，S.T. Kang.(2008). Influence of the ingredients on the compressive strength of UHPC as a fundamental study to optimize the mixing proportion. Proceedings of the second international symposium on ultra high performance concrete，Kassel，105-112.

[13] P. Richard，M. Cheyrezy.(1995). Composition of reactive powder concretes. Cem Concr.Res，(25)：1501-1511.

[14] S. Granger，A. Loukili，G. Pijaudier-cabot，G. Chanvillard.(2005). Mechanical characterization of self-healing effect of cracks in ultra high performance concrete (UHPC). Proceedings of 3rd international conference on construction materials, performance, innovations and structural implications，Vancouver，August：22-24.

[15] R. Bornemann，M. Schmidt，E. Fehling，et al.(2001). Ultra-Hochleistungsbeton UHPC.Beton- und Stahlbetonbau，96，(7)：458-467.

[16] Urs Müller，Meng B，HansCarsten Kühne，et al.(2008). Micro texture and mechanical properties of heat treated and autoclaved Ultra High Performance Concrete (UHPC). International Symposium on Ultra High Performance Concrete.

[17] Sung-Hoon K，Ji-Hyung L，Sung-Gul H，et al.(2017). Microstructural Investigation of Heat-Treated Ultra-High Performance Concrete for Optimum Production. Materials，10(9)：1106.

[18] Fehling E，Schmidt M，Teichmann T，et al.(2005). Dauerhaftigkeit und Berechnung ultrahochfester Betone (UHPC).DFG-Forschungsbericht, Schriftenreihe Baustoffe und Massivbau, Structural Materials and Engineering Series，pp.1.

[19] B. Graybeal.(2008). UHPC in the U.S. highway transportation system, in:

Proceedings of the Second International Symposium on Ultra High Performance Concrete, Kassel University Press GmbH，Kassel，Germany，pp.11.

[20] RebentrostM，Wight G，Fehling E.(2008). Experience and applications of ultra-high performance concrete in Asia. Proceedings of the 2nd International Symposium on Ultra-High Performance Concrete，Kassel University Press GmbH，Kassel，Germany，pp.19-30.

[21] Yang J，Peng G F，Gao Y X，et al.(2014). Mechanical Properties and Durability of Ultra-High Performance Concrete Incorporating Coarse Aggregate. Key Engineering Materials，629-630，96-103.

[22] Li Y J，Gong Y L，Yin J.(2011). Strength and Durability of High Performance Road Concrete Containing Ultra-Fine Fly Ash. Applied Mechanics and Materials，99-100，1264-1268.

[23] Kusumawardaningsih Y，Fehling E，Ismail M.(2015). UHPC Compressive Strength Test Specimens: Cylinder or Cube?. Procedia Engineering，125：1076-1080.

[24] Jin Liu，Yu Wenxuan，Du Xiuli，et al.(2019). Meso-scale modelling of the size effect on dynamic compressive failure of concrete under different strain rates. International Journal of Impact Engineering，125: 1-12.

[25] National Standard of the People's Republic of China.(2015). Reactive Powder Concrete GB/T 31387-2015. Beijing：China Standard Press.

[26] Zheng WZ，Li L.(2009). Preparation and Mix Proportion Calculation of Reactive Powder Concrete. Journal of Hunan University(Natural Sciences)，(02)：13-17.

[27] Lu Xinying.(1997). APPlication of the Nernst-Einstein equation to concrete. Cement and Concrete Research，27(2)：293-302.

[28] Deng JF，Fan KN.(1992). Physical chemistry. Beijing：Higher Education Press.